Title

Inhibition of Src Family Kinases Protects Hippocampal Neurons and Improves Cognitive Function after Traumatic Brain Injury

Journal

Journal of Neurotrauma, 31(14)

ISSN

0897-7151

Authors

Liu, Da Zhi

Sharp, Frank R

Van, Ken C

et al.

Publication Date

2014-07-15

DOI

10.1089/neu.2013.3250

Peer reviewed

JOURNAL OF NEUROTRAUMA 31:1268–1276 (July 15, 2014)

DOI: 10.1089/neu.2013.3250

Inhibition of Src Family Kinases Protects Hippocampal Neurons and Improves Cognitive Function after Traumatic Brain Injury

Da Zhi Liu,[1] Frank R. Sharp,[1] Ken C. Van,[2] Bradley P. Ander,[1] Rahil Ghiasvand,[2] Xinhua Zhan,[1] Boryana Stamova,[1] Glen C. Jickling,[1] and Bruce G. Lyeth[2]

Abstract

Traumatic brain injury (TBI) is often associated with intracerebral and intraventricular hemorrhage. Thrombin is a neurotoxin generated at bleeding sites fater TBI and can lead to cell death and subsequent cognitive dysfunction via activation of Src family kinases (SFKs). We hypothesize that inhibiting SFKs can protect hippocampal neurons and improve cognitive memory function after TBI. To test these hypotheses, we show that moderate lateral fluid percussion (LFP) TBI in adult rats produces bleeding into the cerebrospinal fluid (CSF) in both lateral ventricles, which elevates oxyhemoglobin and thrombin levels in the CSF, activates the SFK family member Fyn, and increases Rho-kinase 1(ROCK1) expression. Systemic administration of the SFK inhibitor, PP2, immediately after moderate TBI blocks ROCK1 expression, protects hippocampal CA2/3 neurons, and improves spatial memory function. These data suggest the possibility that inhibiting SFKs after TBI might improve clinical outcomes.

Key words: cognitive memory deficits; hemorrhage; Src family kinases (SFKs); thrombin; traumatic brain injury (TBI)

Introduction

Traumatic brain injury (TBI) occurs in approximately 1.7 million persons each year in the United States and remains the leading cause of death and disability.[1] Emergency care focuses on stabilizing the patient and preventing secondary injury.[2] Once stabilized, surgical treatment may be used to remove hematoma and control intracranial pressure.[2] There are currently no Food and Drug Administration approved drug treatments for TBI, however. Because little can be done to reverse the initial damage caused by TBI,[2] studying early events after the trauma that contribute to cognitive impairment may provide therapeutic targets for treatment of patients with TBI.

TBI is often associated with intracranial hemorrhage (ICH), with blood leaking from ruptured vessels into contused brain parenchyma. Depending on the amount of bleeding and the location and integrity of the ventricle wall, the blood can extend into the ventricular system, leading to traumatic intraventricular hemorrhage (IVH).[3–5] Traumatic IVH is associated with high morbidity and mortality.[6–9]

The lateral fluid percussion (LFP) model is one of the most commonly used rodent models of TBI, in part because of its reproducibility.[10] This model produces both focal and diffuse (mixed) type brain injury by rapidly injecting fluid above the intact dural surface through a craniotomy.[11] Traumatic pathology in the LFP model includes cortical contusion and hemorrhage, cytotoxic and vasogenic brain edema, and spatial memory deficits.[10–14]

Initial tissue response to bleeding is activation of the coagulation cascade, in which thrombin is rapidly released and blood clot formation limits bleeding.[3–5] Large amount of ICH has been associated with increased mortality after TBI.[4] This suggests that the amount of bleeding substantially affects the outcome of patients with TBI.

Thrombin, generated by proteolysis of its precursor prothrombin, participates in the process of blood coagulation and is an essential clotting factor. In addition, thrombin acts on endogenous receptors (protease-activated receptors, PARs)[15–18] that mediate thrombin signaling.[19] Increasing evidence indicates that thrombin, whether in brain parenchyma or the cerebral ventricular system, is a major contributor to brain injury.[5,20–26] Our previous studies have demonstrated that intracerebral injection of thrombin into the rat striatum resulted in a hematoma around which brain edema develops,[25] while intraventricular injection of thrombin disrupted the blood–brain barrier (BBB) and produced brain edema.[26]

Even though inhibiting PARs decreases thrombin-induced brain injury,[23] PAR inhibitors may not be good treatment targets to block thrombin-induced neurotoxicity because they could affect the clotting function of thrombin and cause catastrophic brain

[1]Department of Neurology and the M.I.N.D. Institute, University of California, Davis, Medical Center, Sacramento, California.
[2]Department of Neurological Surgery, University of California, Davis, Davis, California.

hemorrhage post-TBI.[27,28] PARs modulate several intracellular molecules including Src family kinases (SFKs). SFKs consist of at least eight family members, including c-Src, c-Yes, Fyn, Lck, Lyn, Hck, Blk and c-Fgr.[29] SFKs activation results in cell death via multiple mechanisms, such as downstream RhoA- Rho-kinase 1(ROCK) pathway,[30–32] N-methyl-D-aspartate (NMDA) receptor-mediated neurotoxicity,[33–39] aberrant cell cycle reentry,[25,33–42] and others. Unlike anti-thrombin treatments that have potential to cause catastrophic brain hemorrhage post-TBI,[27] inhibiting SFKs has limited effects on hemostasis,[28] because SFKs do not associate with integrin complexes until after platelet aggregation mediated by $\alpha_{IIb}\beta_3$.[28]

Our previous studies have shown that (1) SFK activity increases after ICH,[25,43] and (2) the SFK inhibitors, PP1 or PP2, can attenuate thrombin-induced hematoma, motor deficits, BBB disruption, and brain edema in both rodent intracerebral and intraventricular fresh blood and/or thrombin models.[25,26,43] In this study, we postulated that thrombin that diffuses throughout the brain after release into the cerebrospinal fluid (CSF) can contribute to brain injury via activation of SFKs after TBI, and that inhibition of SFKs may block thrombin-induced neurotoxicity after TBI. To address these hypotheses, we measured oxyhemoglobin and thrombin concentrations in CSF as well as Fyn kinase activity (one SFK subtype), and ROCK1 expression (which is downstream of Fyn) in the hippocampus after LFP-induced TBI. Because hippocampal CA2/3 pyramidal neurons are needed for spatial learning and memory,[44] we examined the numbers of NeuN immunoreactive CA2/3 pyramidal neurons in the hippocampus and assessed spatial memory function after TBI in animals administered a systemic SFK inhibitor, PP2, compared with vehicle controls.

Methods

Subjects

All experimental animal procedures were performed in accordance with National Institutes of Health guidelines and were reviewed and approved by the University of California, Davis Institutional Animal Care and Use Committee. Male Sprague-Dawley rats ($n = 56$ total), weighing 300–350 g, were used in this study. The animals were allowed free access to food and water and were maintained on a 12 h light/12 h dark cycle. After TBI or sham surgery, animals were either underwent CSF sampling or received treatment (drug or vehicle) and allowed to survive for either 24 h or 16 days.

LFP

Experimental TBI was produced with a fluid percussion device (VCU Biomedical Engineering, Richmond, VA)[45] using the lateral orientation.[46] Rats were initially anesthetized with 4% isoflurane (Minrad, New York, NY), intubated, and placed in a stereotaxic frame (Kopf Instruments, Tujunga, CA). They were ventilated with a rodent volume ventilator (Harvard Apparatus model 683, Holliston, MA) and maintained with 2% isoflurane. Depth of anesthesia was monitored every 10 min by testing for suppression of hindpaw withdrawal in response to a toe pinch. Sterile techniques were used during surgery.

Rats were mounted in a stereotaxic frame, a scalp incision made along the midline, and a 4.8-mm diameter craniotomy performed with a trephine on the right parietal bone (4.5 mm posterior to bregma and 3.0 mm lateral to the sagittal suture). Care was taken to ensure that the dura remained intact. A rigid plastic injury tube (modified Luer-Loc needle hub, 2.6 mm inside diameter) was glued over the craniectomy with cyanoacrylate adhesive. Two skull screws (2.1 mm diameter, 6.0 mm length) were placed into burr holes, 1 mm rostral to bregma and 1 mm caudal to lambda. The assembly was secured to the skull with cranioplastic cement (Plastics One, Roanoke, VA). Rectal temperature was continuously monitored and maintained within normal ranges (37 ± 0.5°C) during surgical preparation by a feedback temperature controller pad (CWE model TC-1000, Ardmore, PA). Temporalis muscle temperature was measured just before and after injury by insertion of a 29-gauge needle temperature probe (Physitemp unit TH-5, probe MT-29/2, Clifton, NJ) between the skull and temporalis muscle.

The fluid percussion device consisted of a Plexiglas cylindrical reservoir filled with isotonic saline. One end of the reservoir has a Plexiglas piston mounted on O-rings. The opposite end consists of a transducer housing ending with a 2.6 mm outer diameter male Luer-Lok. The rats were then connected to the fluid percussion device via the Luer-Lok system. Brain injury was induced by the descent of the pendulum from a known height striking the piston of the saline-filled reservoir, forcing a fluid bolus (~ 0.1 mL) into the closed cranial cavity and producing a brief displacement and deformation of brain tissue. After connecting the injury tube to the fluid percussion device, a moderate fluid percussion pulse was delivered within 10 sec. The resulting pressure pulse was measured in atmospheres by an extracranial transducer (model SPTmV0100PG5W02; Sensym ICT, Milpitas, CA) and recorded on a digital storage oscilloscope (model TDS 1002; Tektronix Inc., Beaverton, OR). Sham control animals were surgically prepared and interfaced with the device but with no pressure pulse delivered to the brain.

The plastic injury tube and skull screws were removed and the scalp incision sutured. The animal was disconnected from the ventilator after spontaneous breathing was observed and transferred to a heating pad. Assessment of the righting reflex was performed by placing the rat in a supine position at regular intervals (~ 20 sec). The time required for righting from the supine to the prone position was used as an additional indicator of injury severity.

CSF and hippocampal tissue collection

Rats ($n = 24$) were divided into three groups. The CSF was drawn at 0.5 h post-surgery from sham rats, and CSF was drawn at 0.5 h and 3.0 h post-injury from rats with TBI. We developed a CSF collection method with slight modifications from previous reports.[47–49] Briefly, the anesthetized rat was placed in the stereotaxic frame, and its head was angled downward at approximately 45 degrees from the horizontal plane. After the exposure of the translucent dura mater at the cranial-cervical junction, a 28-gauge needle with a blunt end connected to a 1 mL insulin-filled syringe via 30 cm polyethylene tubing (inner diameter: 0.381 mm) was carefully inserted at a 90-degree angle to the dura mater. As the needle passed through the dura mater into the cisterna magna, gentle negative pressure was created by pulling the syringe plunger to draw approximately 70–120 μL CSF from rats with TBI or 150–210 μL CSF from sham surgery rats. The tubing was then cut and the CSF was transferred into a 0.5 mL centrifuge tube and centrifuged for 10 min at $500 \times g$ at 4°C. The supernatant was aliquoted, frozen in powdered dry ice, and stored at -70°C.

Immediately after removing the CSF, the rats were transcardially perfused with saline to wash out the blood in the vasculature. Hippocampi ipsilateral to the injury were dissected, frozen in liquid nitrogen, and stored at a -70°C.

Assessment of thrombin in CSF

The CSF samples (50 μL for each assay) and all reagents of the Fluorimetric 520 Thrombin Assay Kit (AnaSpec, Fremont, CA) were warmed to room temperature. Rat thrombin (Sigma, St. Louis, MO) was diluted (5, 2.5, 1.25, 0.625, 0.3125, 0 μg/mL) for standards. The manufacturer's protocol was followed, and reagents

were mixed with each CSF sample in a well of a black 96 well plate (Midland Scientific, Omaha, NE) and incubated for 60 min at room temperature. A stop solution terminated the reaction, and fluorescence intensity was measured at Excitation/Emission = 490 nm/520 nm. Statistical differences were determined using one-way analysis of variance ANOVA followed by the Tukey *post hoc* test.

Measurement of oxyhemoglobin in CSF

The CSF samples and standards (1 μL for each assay) were measured at 350–600 nm using a NanoDrop-2000 spectrophotometer (Thermo Sci., Wilmington, DE). The absorbance value at 415 nm of each sample was measured. Human oxyhemoglobin (Calzyme, San Luis Obispo, CA) was diluted as a standard (1, 0.5, 0.25, 0.125, 0.0625, 0 mg/mL). Statistical differences were determined using one-way ANOVA followed by the Tukey *post hoc* test.

Fyn kinase activity assay

The rat hippocampal samples were homogenized and protein isolated in extraction buffer (Clontech Laboratory, Inc., Mountain View, CA). Our preliminary studies indicated Fyn was the primary SFK family member activated after TBI, so Fyn kinase activity was measured. Fyn protein was immunoprecipitated with a Fyn antibody (Santa Cruz Biotechnology, Inc., Dallas, TX), washed three times in phosphate buffered saline (PBS) with 0.5% Tween-20 (PBST), and resuspended in kinase reaction buffer, optimized to preserve Fyn enzymatic activity. The immunoprecipitated Fyn kinase was assayed for activity using the Universal Tyrosine Kinase Assay Kit (Clontech Laboratory, Inc., Mountain View, CA). Statistical differences were determined using one-way ANOVA followed by the Tukey *post hoc* test.

Treatment groups for acute and chronic study

Rats ($n = 16$) were divided into three groups (4–6 rats/group) for the acute study. The non-specific SFK inhibitor PP2 (4-amino-5-(4-chlorophenyl)-7-(t-butyl)pyrazolo[3,4-d]pyrimidine, Calbiochem, Billerica, MA) was dissolved in dimethyl sulfoxide (DMSO) (5 mg/mL), and diluted 20 times in saline before intraperitoneal injection. One group of rats received two intraperitoneal injections of PP2 (2.0 mg/kg, one injection was immediately after TBI, and the second injection at 3 h post-TBI). The remaining two groups of rats (TBI or sham surgery) received two intraperitoneal injections of vehicle (5% DMSO in saline) using the same time interval as PP2 administration. Twenty-four hours after TBI, the rats were euthanized, and brains were removed for either immunohistochemistry staining or Western blots.

Rats ($n = 24$) were divided into three groups (5–9 rats/group) for the chronic study. The three groups of rats received the same TBI surgery and treatment (either PP2 or vehicle) as in the acute study, except that these animals were sacrificed on day 16 and spatial memory function was assessed using the Morris water maze (MWM) on days 12 through 16.

Protein extraction and Western blot

ROCK1 protein expression was assessed because it is a downstream target of SFKs, including Fyn. Rats were euthanized at 24 h after surgery, and ipsilateral hippocampi were processed for Western blot analysis. Equal amounts of protein (50 μg) were loaded onto polyacrylamide-SDS gels, separated by electrophoresis, and then transferred to nitrocellulose membranes. After a brief rinse in PBST, the membranes were incubated with 5% dry milk in PBS for 1 h, and then incubated with rabbit anti-rat ROCK1 antibody (1:500, Abcam) overnight at 4°C. Mouse anti-rat glyceraldehyde 3-phosphate dehydrogenase antibody (1:1,000, Santa Cruz) was used as the internal control. After three 10 min rinses in PBST, the membranes were incubated with horseradish peroxidase-conjugated anti-rabbit or anti-mouse immunoglobulin G (1:5,000, Bio-Rad, CA). After three more 10 min rinses in PBST, bands on the membranes were visualized using the enhanced chemiluminescent detection system (Thermo Sci.). Quantification was performed by optical density methods using the ImageJ software (NIH). Statistical differences were determined using the unpaired *t* test.

MWM

Acquisition of spatial learning and memory was assessed in the MWM on days 12–16 after TBI.[50] The test apparatus consisted of a large white circular tank (220 cm diameter by 60 cm high) filled with water to a depth of 22 cm. Water temperature was maintained at 24–28°C. A transparent circular escape platform (12.8 cm diameter, 20 cm high) was placed in a fixed position in the tank 2 cm below the water surface. Four consistent visual cues were located in the test room outside of the maze. Rats were released from one of four starting points (selected randomly on each day for each rat) and allowed 120 sec to find and mount the escape platform. If the rat did not find the platform within 120 sec, the experimenter placed the rat on the platform. The rat remained on the platform for 30 sec before being removed from the maze. The rat received a 4-min intertrial interval in a warmed holding cage before being returned to the maze for subsequent trials. Rats received a total of four trials per day, one from each starting point, over 5 consecutive days.

Mean latency to find the platform was calculated for each day to assess learning. Data from all trials were recorded using a video tracking system (Poly-Track Video Tracking System version 2.1, San Diego Instruments Inc. San Diego, CA). Statistical differences were determined using repeated measures ANOVA with assessment days as the repeated variable within subjects followed by the Dunnett *post hoc* test.

Brain sample preparation and immunohistochemistry

Rats were anesthetized with 3% isoflurane and transcardially perfused with saline followed by 4% paraformaldehyde. Brains were removed, post-fixed 2–6 hours, and placed in 30% sucrose in PBS. The fixed rat brains were embedded in frozen section medium and mounted on the microtome. Coronal sections (50 μm) were cut on a freezing microtome and stored at -20°C in a cryoprotectant composed of 30% glycerol, 20% ethylene-glycol and 50% PBS. Some representative images of control and TBI brains were taken during sectioning to show the distribution of blood in the parenchyma and ventricles of animals with TBI.

The avidin-biotin-peroxidase complex (Vectastain Elite ABC Kit, Vector Laboratories, Inc., Burlingame, CA) method was used to perform NeuN (a marker of mature neurons) immunohistochemistry. Brain sections were incubated at room temperature in 0.3% H_2O_2 in methanol for 30 min to quench endogenous peroxidase. After two 5 min rinses in PBS, sections were incubated with 3% horse blocking serum for 20 min and then incubated for 0.5 h in primary antibody (mouse anti-NeuN, 1:150, Millipore MAB377, Billerica, MA) diluted in PBS containing 0.1% Triton X-100 and 3% horse serum. After being washed in PBS, sections were incubated in biotinylated secondary antibody (goat anti-mouse 1:1,000, Vector BA 9200, Burlingame, CA) for 0.5 h. After three 5 min rinses in PBS, sections were placed in Vectastain ABC reagent for 0.5 h. After two more 5 min washes, sections were incubated in peroxidase substrate 3, 3′-diaminobenzidine (DAB) solution for 10 min. DAB staining was examined using a Nikon E600 microscope.

Stereological cell counts

The NeuN-positive cell counts were performed on a microscope (Nikon E600, Nikon, Tokyo) with a motorized stage (Bioprecision2, Ludl Electronic Products, Inc., Hawthorne, NY) using computer software (Stereo Investigator™ 8.0, Microbrightfield, Inc., Williston, VT).

The total number of NeuN-positive pyramidal neurons in the CA2/3 region of the hippocampus was quantified using stereological methods. Serial sections cut at 50 μm thick were collected at bregma −2.80 mm to bregma −4.16 mm for a total of 10 sections per brain. Briefly, the border of CA2/3 of the brain was outlined using a 4×objective. A 100×oil immersion objective (1.4 numerical aperture) with oil condenser was used for cell counting. Dissectors separated by 150 μm are randomly, systematically, and uniformly placed throughout the outlined region by the software. The NeuN-positive neurons were counted if the soma fell within the counting frame or were on the inclusion line. The dissector height was 10 μm and the guard height was 0.4 μm.

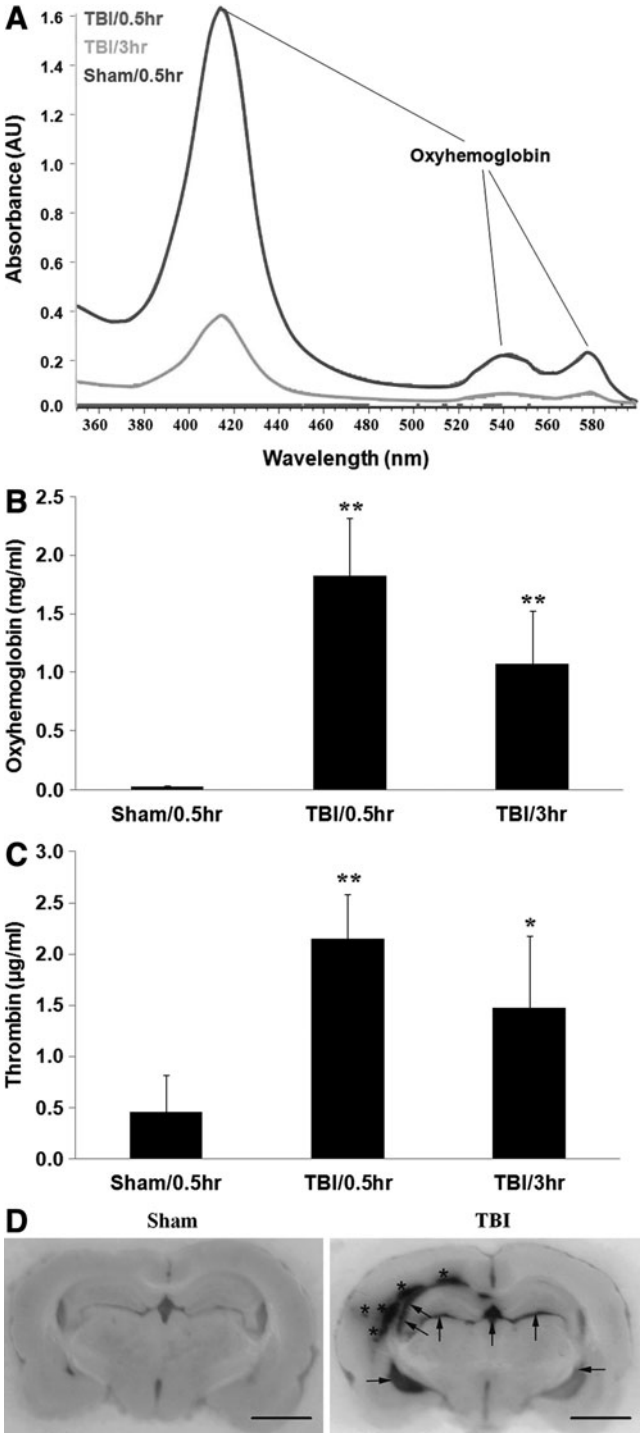

Estimated numbers of the NeuN-postive neurons in the target brain region were generated by the Stereologer software using the following equation: $N_{obj} = (\sum N)(1/SSF)(1/ASF)(1/TSF)$.[51] In this equation $\sum N_{obj}$ indicates the sum of objects sampled in the sections, SSF indicates the section sampling fraction, ASF indicates the area sampling fraction, and TSF indicates the thickness sampling fraction. Statistical differences were determined using unpaired *t* test.

Results

Oxyhemoglobin in CSF after TBI

A typical spectrophotometric scan of CSF samples from rats with TBI showed that oxyhemoglobin peaked at 0.5 h (Fig. 1A, red line) and decreased at 3 h (Fig. 1A, orange line), but was still higher than sham control (Fig. 1A, purple line). The peak at 415 nm was the main peak indicating the presence of oxyhemoglobin in the CSF samples, with two secondary peaks at ∼540 nm and ∼580 nm (Fig. 1A), which are distinguishable from derivatives of hemoglobin including methemoglobin. The amount of oxyhemoglobin in rat CSF increased at 0.5 hour (Fig. 1B; 1.82 ± 0.49 μg/mL [TBI/0.5 h] vs. 0.03 ± 0.004 mg/mL [sham/0.5 h], $^{**}p < 0.01$), and at 3 h (Fig. 1B; 1.07 ± 0.45 mg/mL [TBI/3 h] vs. 0.03 ± 0.004 mg/mL [sham/0.5 h], $^{**}p < 0.01$) after TBI.

Thrombin concentration in CSF after TBI

Thrombin concentration in rat CSF increased at 0.5 h (Fig. 1C; 2.15 ± 0.43 μg/mL [TBI-0.5 h] vs. 0.45 ± 0.37 μg/mL [sham], $^{**}p < 0.01$), and at 3 h (Fig. 1C; 1.48 ± 0.70 μg/mL [TBI-3 h] vs. 0.45 ± 0.37 μg/mL [sham], $^{*}p < 0.05$) after TBI. The data also showed that thrombin decreased at 3 h in comparison with that at 0.5 h after TBI, but not signifigantly (Fig. 1C).

Hemorrhage distribution in brain after TBI

As shown in Figure 1D, hemorrhage was observed after TBI in ipsilateral parenchyma (marked with stars) and lateral ventricles

FIG. 1. Cerebroventricular oxyhemoglobin is increased after experimental traumatic brain injury (TBI). (**A**) Representative absorbance curve of oxyhemoglobin in cerebrospinal fluid (CSF) at 0.5 h after sham control surgery, and 0.5 h and 3 h after TBI. The highest peak for oxyhemoglobin was observed at 415 nm, and secondary, much smaller peaks are observed between 525–600 nm. Top line: TBI–0.5 h; middle line: TBI–3 h; bottom line: sham. (**B**) Oxyhemoglobin peaked at 0.5 h, and decreased at 3 h in comparison with that at 0.5 h after TBI. The Y-axis shows oxyhemoglobin concentration (mg/mL). Each column represents the mean ± standard error. $^{**}p < 0.01$, vs. sham control (one-way analysis of variance (ANOVA) followedby the Tukey *post hoc* test). (**C**) Thrombin concentration is increased after experimental TBI. Thrombin concentration in CSF peaked at 0.5 h, and decreased at 3 h in comparison with that at 0.5 h after TBI. The Y-axis shows thrombin concentration (μg/mL). Each column represents the mean ± standard error. $^{**}p < 0.01$, $^{*}p < 0.05$ vs. sham control (one-way ANOVA followed by the Tukey *post hoc* test). (**D**) Brain hemorrhage in ipsilateral parenchyma (marked with stars) and bilateral cerebral ventricles (marked with arrows) at 24 h after TBI. Rats were transcardially perfused with saline followed by 4% paraformaldehyde 24 h after sham surgery or TBI. The fixed rat brains were embedded in frozen section medium and mounted on the microtome. The representative images were taken before the sections were cut off. Scale bars: 6.25 mm.

(marked with arrows) at 24 h after TBI. Ventricular hemorrhage was greater in ipsilateral than contralateral ventricles.

Fyn activity in hippocampi after TBI

Fyn kinase activity in hippocampi increased at 0.5 h (Fig. 2; 99.4 ± 11.9 mU/mL [TBI/0.5 h] vs. 49.3 ± 6.6 mU/ml [sham], $^{**}p < 0.01$) and decreased to control levels at 3 h (Fig. 2; 49.5 ± 28.1 mU/mL [TBI/3h] vs. 99.4 ± 11.9 mU/mL [TBI/0.5 h], $^{\#}p < 0.05$) after TBI. There were no significant differences of Fyn activity between TBI/3 h and sham (Fig. 2).

The effects of PP2 on ROCK1 protein expression in hippocampi after TBI

ROCK 1 protein expression in hippocampi ipsilateral to injury increased 2.15 times at 24 h post-TBI (Fig. 3, TBI vs. sham, $^{**}p < 0.01$). PP2 attenuated TBI-induced ROCK1 protein upregualtion (Fig. 3, TBI/PP2 vs. TBI, $^{\#\#}p < 0.01$).

The effects of PP2 on numbers of hippocampal CA2/3 neurons after TBI

Rat brain sections were immunostained using NeuN. In the hippocampus of sham rats, the subdivisions CA1c through CA3c were shaped in a tight U (Fig. 4A,G), shown as a single layer of densely packed 5–6 $NeuN^+$ pyramidal cells deep (Fig. 4B, H). We observed that CA2/3 neurons were decreased at 1 day (Fig. 4C, D) and 16 days (Fig. 4I, J) after TBI. The SFK inhibitor PP2 attenuated TBI-induced CA2/3 neuron loss at both 1 day (Fig. 4E, F) and 16 days (Fig. 4K, L) after TBI.

Quantification of $NeuN^+$ neuronal cell counts showed that the number of $NeuN^+$ cells decreased in the vehicle TBI group compared with sham surgery control (Fig. 4M, vehicle vs sham, $p < 0.05$). Treatment of TBI animals with the SFK inhibitor PP2 increased the number of $NeuN^+$ neuronal cells in the PP2 group compared with the vehicle group in the ipsilateral CA2/3 region of hippocampus at 16 days after TBI (Fig. 4M, PP2 vs. vehicle, $p < 0.05$).

The effects of PP2 on cognitive function after TBI

There was a significant effect of group on latency to find the platform in the MWM ($F_{(2,19)} = 6.6$, $p < 0.01$; Fig. 5). The TBI/vehicle group had significantly longer latencies to find the hidden platform over the 5 days of testing compared with the sham group ($p < 0.01$) (Fig. 5). Treatment with PP2 significantly improved performance compared with the vehicle treated TBI group ($p < 0.05$) (Fig. 5).

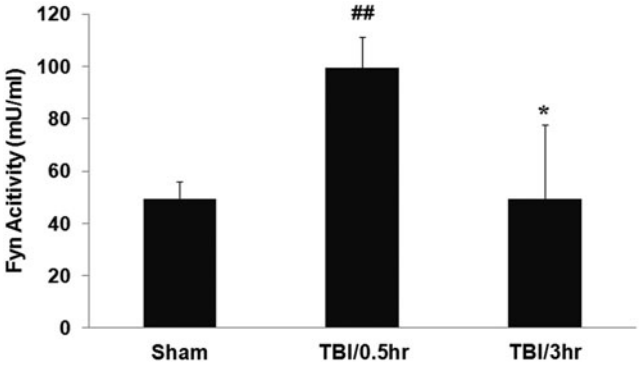

FIG. 2. Fyn kinase activity is increased after experimental TBI. Fyn activity in hippocampi peaked at 0.5 h, and returned to sham control levels at 3 hrs after TBI. The Y-axis shows Fyn activity (mU/ml). Each column represents the mean ± standard error. $^{\#\#}p < 0.01$ vs. sham control, $^{*}p < 0.05$ *vs* TBI/0.5 h (one-way ANOVA followed by Tukey's *post hoc* test).

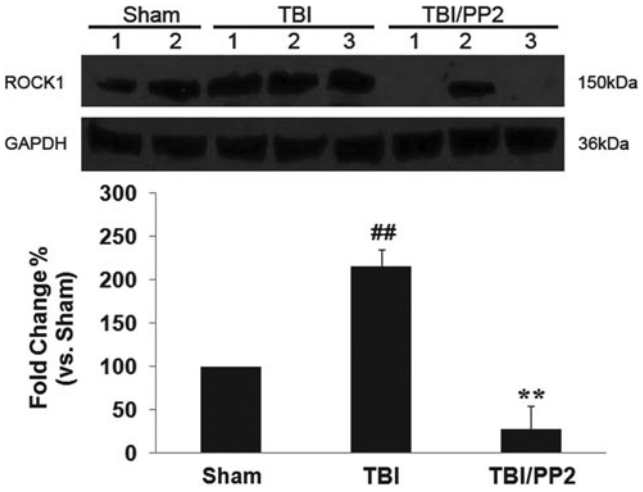

FIG. 3. Src family kinase inhibitor PP2 attenuates Rho-kinase 1 (ROCK1) protein expression at 24 h post-TBI. Upper panel: Western blots of ROCK1 and glyceraldehyde 3-phosphate dehydrogenase (GAPDH) expression 24 h after TBI; lower panel: quantification of ROCK1 protein expression in each group. Each column represents the mean ± standard error. $^{**}p < 0.01$ vs. sham, $^{\#\#}p < 0.01$ vs. traumatic brain injury (TBI) (unpaired *t* test).

Discussion

This study demonstrated that moderate LFP injury TBI in adult rats resulted in blood in the ventricles that was associated with elevated oxyhemoglobin, elevated thrombin levels in the CSF, activation of the SFK family member Fyn, and up-regulation of the Fyn regulated ROCK1 protein. TBI was associated with decreased numbers of neurons in CA2/3 of the hippocampus and deficits in spatial memory function in the MWM. Both the hippocampal cell loss and spatial memory deficits were significantly attenuated by the SFK inhibitor PP2. These data suggest the possibility that inhibiting SFKs after TBI might improve clinical outcomes.

This study was initiated in part by our observations that the CSF was often red or pink at early times after LFP in rats. The observations of bloody CSF were consistent with histological data showing hemorrhage not only in the ipsilateral parenchyma but also in the ventricles 24 h post-TBI. Thus, IVH was a consistent feature of the LFP-induced TBI model used here. This was also supported by our data showing that oxyhemoglobin was increased compared with controls at 0.5 h and 3 h in the CSF after LFP-induced TBI. Hemoglobin itself can be neurotoxic, because it can lead to the release of reactive oxygen species (ROS) including superoxide anion and hydrogen peroxide.[52,53]

An initial tissue response to bleeding is activation of the coagulation cascade, in which thrombin is rapidly released and blood clotting is initiated to limit bleeding.[3–5] Therefore, we hypothesized that the concentration of thrombin should increase in the CSF when bleeding extended into the ventricles. Our data showed that thrombin increased approximately five-fold at 0.5 h and three-fold at 3 h in the CSF after moderate LFP-induced TBI in rats. These data confirmed that bleeding extended into the cerebral ventricles

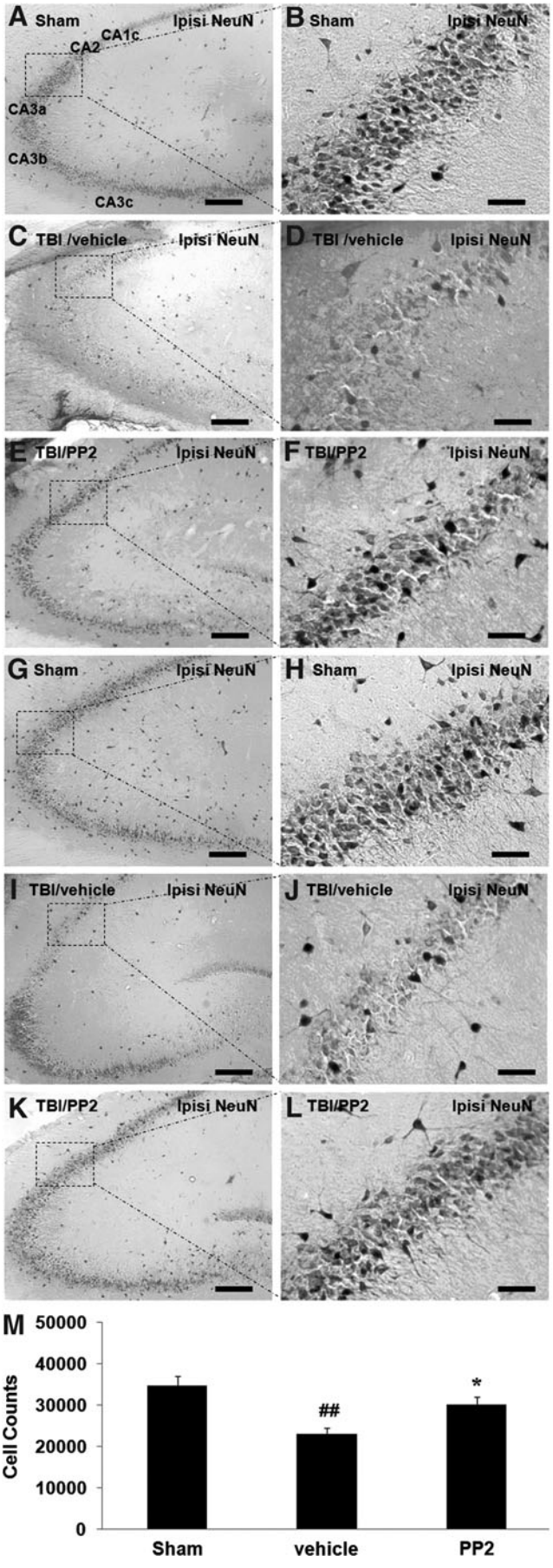

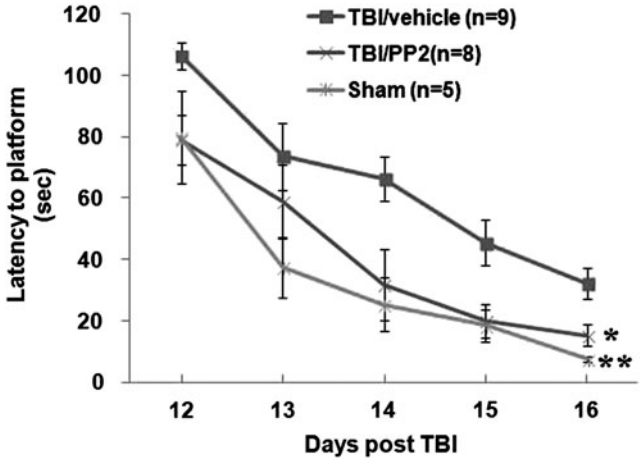

FIG. 5. PP2 reduced traumatic brain injury (TBI)-induced cognitive deficits. Cognitive function was examined at 12 through 16 days after the experimental TBI using the Morris Water Maze. The Y-axis shows latency to finding platform (sec). Each point represents the mean ± standard error. Top line: vehicle-treated TBI (TBI/vehicle); middle line: PP2-treated TBI (TBI/PP2); bottom line: sham control (sham/vehicle). (#$p < 0.05$, ##$p < 0.01$ [TBI/vehicle] vs. [sham/vehicle]; *$p < 0.05$, **$p < 0.01$ [TBI/PP2] vs. [TBI/vehicle]) (repeated measures analysis of variance followed by Dunnett *post hoc* test).

in this rat moderate LFP-induced TBI model resulting in traumatic IVH, which is frequently associated with human TBI.

The results of this study suggest the possibility that thrombin activation of SFKs contributes to these spatial memory deficits, because inhibiting SFKs prevented the TBI-induced spatial memory deficits. This hypothesis is based on results from the current and previous studies. A number of studies have documented that high concentration of thrombin causes brain injury.[5,20–26] The increased thrombin observed in the CSF after TBI in this study can diffuse throughout the ventricles and affect brain structures bilaterally, even though the primary TBI impact occurs unilaterally.

As CSF flows through the ventricular system in the brain, it exchanges molecules with the interstitial fluid of the brain parenchyma.[54] In support of this, our previous studies showed that

FIG. 4. Src family kinase (SFK) inhibitor PP2 promotes CA2/3 neuron survival at both 1 day ($n = 2–3$) and 16 days ($n = 5–9$) after traumatic brain injury (TBI). Panel **A** shows the subdivisions CA1c through CA3c in the hippocampus of sham rats, shown as a single layer of densely packed 5–6 $NeuN^+$ cells (pyramidal neurons) deep. Compared with the sham group, $NeuN^+$ cells loss in CA2/3 region at 1 day (panels **C, D**) and 16 days (panels **I, J**) after TBI, and the SFK inhibitor PP2 attenuated TBI-induced CA2/3 neuron loss at both 1 day (panels **E, F**) and 16 days (Panels **K, L**) after TBI. Each right panel shows a higher power image of the area within dashed lines in its left panel. (**M**) Quantification of NeuN stained cells in the ipsilateral CA2/3 region of hippocampus between groups at 16 days after TBI. Fewer $NeuN^+$ cells observed in vehicle group compared with sham surgery control, but more $NeuN^+$ cells observed in the PP2 group compared with the vehicle group. Each right panel shows a higher magnification image of the area within dashed lines in its left panel. Each column represents the mean ± standard error, # $p < 0.05$ compared with sham group; *$p < 0.05$ compared with vehicle group (unpaired *t* test). Scale bars: 200 μm (panels A, C, E, G, I, K); 50 μm (panels B, D, F, H, J, L).

injection of thrombin into one lateral ventricle produced bilateral injury of astrocytes and brain microvascular endothelial cells, BBB disruption, as well as brain edema in both hippocampi and in the brain as a whole.[26] Therefore, it is likely that the increased thrombin in CSF produces injury to the hippocampus and that this likely contributes to the spatial memory deficits observed after LFP in this and other studies.

The results indicate that bleeding into the ventricular system can result in bilateral brain injury mediated by thrombin activation of SFKs, although cortical contusion and hemorrhage are mostly limited to the ipsilateral side after the LFP-induced brain injury.[55,56] This presents a possible mechanism by which unilateral brain injury affects the contralateral hemisphere, leading to cognitive spatial memory deficits that usually require bilateral damage to the hippocampus.

Fyn is one important member of the SFK oncogene family.[57] The Fyn gene shows alternative splicing of the seventh exon encoding the kinase domain, yielding a hematopoietic specific isoform, and another brain specific isoform.[58] *In situ* hybridization analysis showed that Fyn mRNA was specifically expressed in neurons of embryos and newborn mice, and expressed in oligodendrocytes as well as neurons in adult mice.[59] In the current study, we found that Fyn kinase activity increased almost twofold after moderate LFP-induced TBI. This finding provided the rationale for testing whether a SFK inhibitor (PP2) would improve histological and cognitive outcomes in this TBI model.

In this study, we showed that the released thrombin and Fyn kinase were both activated at the early time post-TBI. This was consistent with our hypothesis that thrombin release leads to activation of SFKs including Fyn. Fyn activity returned to basal level, however, whereas the thrombin activity was still up at 3 h post-TBI. The different time frames of Fyn and thrombin suggested they were inactivated and/or eliminated differently post-TBI. For example, ROS generated by oxyhemoglobin autooxidation post-TBI can inactivate Fyn activity.[60] In addition, SFKs can initiate negative feedback to prevent their sustained activation through recruitment of inhibitory factor C-terminal Src (Csk).[61] The feedback loop consists of a few steps: SFKs activation leads to phosphorylation of Csk binding protein (Cbp), and the phosphorylated Cbp targets Csk to SFKs and promotes inhibitory Csk phosphorylation of SFKs.[62] In contrast, thrombin inactivation associates with CSF circulation and endogenous antithrombin factors in the CSF post-TBI.[63]

In light of the fact that the SFK genes belong to oncogenes that are associated with cell proliferation, neuronal differentiation, and other important cellular processes, chronic silencing of these SFK genes could lead to serious side effects.[64–66] Our previous studies investigated the time window of PP2 administration after thrombin intracerebroventricular injection, and have found that (1) acute PP2 administration immediately after ventricular thrombin injections attenuated BBB disruption and brain edema during the acute stage of the thrombin-induced brain injury; and (2) delayed and lasting PP2 administration, given on day 2 though day 6 after ventricular thrombin injections, prolonged BBB disruption and brain edema during the recovery stage of the thrombin-induced brain injury.[26] This suggests that delayed and lasting SFK inhibition might diminish the repair processes after thrombin-induced brain injury. Therefore, we designed the current study so that SFK inhibition with PP2 was given during the acute stage post-TBI. The data show that acute treatment with the SFK inhibitor, PP2, decreased CA2/3 neuron loss at 16 days and attenuated cognitive deficits at 16 days after moderate LFP-induced TBI in rats.

We also found that the PP2 prevented ROCK1 expression upregulation post-TBI. This might be implicated in the neuroprotective effects of SFK inhibition post-TBI, because SFKs can activate the RhoA-ROCK pathway,[30] which plays critical roles to mediate the death of hippocampal neurons after brain injury in rats.[31,32] Apart from the possible ROCK1 mechanism by which SFKs mediate brain injury, SFKs also phosphorylate NMDA receptors and augment NMDA receptor activity.[33–37] This could lead to cell death after TBI as has been shown for ischemic and hemorrhagic stroke.[26,41,42] In addition, we have previously shown that thrombin activation of SFKs leads to activation of cell cycle genes and programmed neuronal cell death,[25,38–40] which could also be occurring in this TBI model.

There are several limitations to the current study. Apart from thrombin, there may be other potential neurotoxins (e.g., hemoglobin, ROS, glutamate, lactate) released into the CSF after TBI. It is not very clear how these might interact with SFKs to damage the brain after TBI. Although PP2 improved outcomes, and the data showed Fyn kinase activity increases after TBI; the specific SFK members, such as c-Src, Fyn, Lyn, and others were not directly addressed and will need future study.

Acknowledgment

This study was supported by AHA grant 12BGIA12060381 (DZL) and NIH grant NS054652 (FRS).

Author Disclosure Statement

No competing financial interests exist.

References

1. Faul, M., Xu, L., Wald, M., and Coronado, V. (2010). *Traumatic Brain Injury in the United States: Emergency Department Visits, Hospitalizations, and Deaths.* Centers for Disease Control and Prevention, National Center for Injury Prevention and Control: Atlanta. pps. 7–23.
2. National Institute of Neurological Disorders and Stroke. (2013). Traumatic Brain Injury: Hope Through Research. Available at: www.ninds.nih.gov/disorders/tbi/detail_tbi.htm. Accessed April 1, 2014.
3. Gaetz, M. (2004). The neurophysiology of brain injury. Clin. Neurophysiol. 115, 4–18.
4. Perel, P., Roberts, I., Bouamra, O., Woodford, M., Mooney, J., and Lecky, F. (2009). Intracranial bleeding in patients with traumatic brain injury: a prognostic study. BMC Emerg. Med. 9, 15.
5. Keep, R., Hua, Y., and Xi, G. (2012). Intracerebral haemorrhage: mechanisms of injury and therapeutic targets. Lancet Neurol. 11, 720–731.
6. . Atzema, C., Mower, W.R., Hoffman, J.R., Holmes, J.F., Killian, A.J., and Wolfson, A.B. (2006). Prevalence and prognosis of traumatic intraventricular hemorrhage in patients with blunt head trauma. J. Trauma 60, 1010–1017.
7. Badjatia, N., and Rosand, J. (2005). Intracerebral hemorrhage. Neurologist 11, 311–324.
8. Flaherty, M., Haverbusch, M., Sekar, P., Kissela, B., Kleindorfer, D., Moomaw, C.J., Sauerbeck, L., Schneider, A., Broderick, J.P., and Woo, D. (2006). Long-term mortality after intracerebral hemorrhage. Neurology 66, 1182–1186.
9. Fogelholm, R., Murros, K., Rissanen, A., and Avikainen, S. (2005). Long term survival after primary intracerebral haemorrhage: a retrospective population based study. J. Neurol. Neurosurg. Psychiatry 76, 1534–1538.
10. Kabadi, S.V., Hilton, G.D., Stoica, B.A., Zapple, D.N., and Faden, AI. (2010). Fluid-percussion-induced traumatic brain injury model in rats. Nat. Protoc. 5, 1552–1563.
11. Thompson, H.J., Lifshitz, J., Marklund, N., Grady, M.S., Graham, D.I., Hovda, D.A., and McIntosh, T.K. (2005). Lateral fluid percussion brain injury: a 15-year review and evaluation. J. Neurotrauma 22, 42–75.
12. Fedor, M., Berman, R.F., Muizelaar, J.P., and Lyeth, B.G. (2010). Hippocampal theta dysfunction after lateral fluid percussion injury. J. Neurotrauma 27, 1605–1615.

13. Wang, T., Huang, X., Van, K., Went, G., Nguyen, J., and Lyeth, B. (2014). Amantadine Improves cognitive outcome and increases neuronal survival after fluid percussion traumatic brain injury in rats. J. Neurotrauma 31, 370–377.
14. Gurkoff, G.G., Feng, J.F., Van, K.C., Izadi, A., Ghiasvand, R., Shahlaie, K., Song, M., Lowe, D.A., Zhou, J., and Lyeth, B.G. (2013). NAAG peptidase inhibitor improves motor function and reduces cognitive dysfunction in a model of TBI with secondary hypoxia. Brain Res. 1515, 98–107.
15. Vu, T.K., Hung, D.T., Wheaton, V.I., and Coughlin, S.R. (1991). Molecular cloning of a functional thrombin receptor reveals a novel proteolytic mechanism of receptor activation. Cell 64, 1057–1068.
16. Coughlin, S.R., Vu, T.K., Hung, D.T., and Wheaton, V.I. (1992). Expression cloning and characterization of a functional thrombin receptor reveals a novel proteolytic mechanism of receptor activation. Semin. Thromb. Hemost. 18, 161–166.
17. Ishihara, H., Connolly, A.J., Zeng, D., Kahn, M.L., Zheng, Y.W., Timmons, C., Tram, T., and Coughlin, S.R. (1997). Protease-activated receptor 3 is a second thrombin receptor in humans. Nature 386, 502–506.
18. Nakanishi-Matsui, M., Zheng, Y.W., Sulciner, D.J., Weiss, E.J., Ludeman, M.J., and Coughlin, S.R. (2000). PAR3 is a cofactor for PAR4 activation by thrombin. Nature 404, 609–613.
19. Wang, H., and Reiser, G. (2003).Thrombin signaling in the brain: the role of protease-activated receptors. Biol. Chem. 384, 193–202.
20. Xi, G., Reiser, G., and Keep, R. (2003). The role of thrombin and thrombin receptors in ischemic, hemorrhagic and traumatic brain injury: deleterious or protective? J. Neurochem 84, 3–9.
21. Donovan, F.M., Pike, C.J., Cotman, C.W., and Cunningham, D.D. (1997). Thrombin induces apoptosis in cultured neurons and astrocytes via a pathway requiring tyrosine kinase and RhoA activities. J. Neurosci. 17, 5316–5326.
22. Xi, G., Keep, R.F., and Hoff, J.T. (2006). Mechanisms of brain injury after intracerebral haemorrhage. Lancet Neurol. 5, 53–63.
23. Xue, M., Hollenberg, M.D., and Yong, V.W. (2006).Combination of thrombin and matrix metalloproteinase-9 exacerbates neurotoxicity in cell culture and intracerebral hemorrhage in mice. J. Neurosci. 26, 10281–10291.
24. Fujimoto, S., Katsuki, H., Ohnishi, M., Takagi, M., Kume, T., and Akaike, A. (2007). Thrombin induces striatal neurotoxicity depending on mitogen-activated protein kinase pathways in vivo. Neuroscience 144, 694–701.
25. Liu, D.Z., Cheng, X.Y., Ander, B.P., Xu, H., Davis, R.R., Gregg, J.P., and Sharp, F.R. (2008). Src kinase inhibition decreases thrombin-induced injury and cell cycle re-entry in striatal neurons. Neurobiol. Dis. 30, 201–211.
26. Liu, D.Z., Ander, B.P., Xu, H., Shen, Y., Kaur, P., Deng, W., and Sharp, F.R. (2010). Blood-brain barrier breakdown and repair by Src after thrombin-induced injury. Ann. Neurol. 67, 526–533.
27. Garber, S.T., Sivakumar, W., and Schmidt, R.H. (2012). Neurosurgical complications of direct thrombin inhibitors—catastrophic hemorrhage after mild traumatic brain injury in a patient receiving dabigatran. J. Neurosurg. 116, 1093–1096.
28. Thomas, S.M., and Brugge, J.S. (1997). Cellular functions regulated by Src family kinases. Annu. Rev. Cell Dev. Biol. 13, 513–609.
29. Oda, H., Kumar, S., and Howley, P.M. (1999). Regulation of the Src family tyrosine kinase Blk through E6AP-mediated ubiquitination. Proc. Natl. Acad. Sci. U. S. A. 96, 9557–9562.
30. Joshi, A., Dimitropoulou, C., Thangjam, G., Snead, C., Feldman, S., Barabutis, N., Fulton, D., Hou, Y., Kumar, S., Patel, V., Gorshkov, B., Verin, A., Black, S., and Catravas, J. (2013). Hsp90 inhibitors prevent LPS-induced endothelial barrier dysfunction by disrupting RhoA signaling. Am. J. Respir. Cell Mol. Biol. In press. AUTHOR: STILL IN PRESS?
31. Dubreuil, C., Marklund, N., Deschamps, K., McIntosh, T.K., and McKerracher, L. (2006). Activation of Rho after traumatic brain injury and seizure in rats. Exp. Neurol. 198, 361–369.
32. Jeon, B.T., Jeong, E.A., Park, S.Y., Son, H., Shin, H.J., Lee, D.H., Kim, H.J., Kang, S.S., Cho, G.J., Choi, W.S., and Roh, G.S. (2013). The Rho-kinase (ROCK) inhibitor Y-27632 protects against excitotoxicity-induced neuronal death in vivo and in vitro. Neurotox. Res. 23, 238–248.
33. Groveman, B.R., Feng, S., Fang, X.Q., Pflueger, M., Lin, S.X., Bienkiewicz, E.A., and Yu, X. (2012).The regulation of N-methyl-D-aspartate receptors by Src kinase. FEBS J. 279, 20–28.
34. Yu, X.M., Askalan, R., Keil, G.J. 2nd, and Salter, M.W. (1997). NMDA channel regulation by channel-associated protein tyrosine kinase Src. Science 275, 674–678.
35. Salter, M.W., and Kalia, L.V. (2004). Src kinases: a hub for NMDA receptor regulation. Nat. Rev. Neurosci. 5, 317–328.
36. Trepanier, C.H., Jackson, M.F., and MacDonald, J.F. (2012). Regulation of NMDA receptors by the tyrosine kinase Fyn. FEBS J. 279, 12–19.
37. Choi, U.B., Xiao, S., Wollmuth, L.P., and Bowen, M.E. (2011). Effect of Src kinase phosphorylation on disordered C-terminal domain of N-methyl-D-aspartic acid (NMDA) receptor subunit GluN2B protein. J. Biol. Chem. 286, 29904–29912.
38. Liu, D.Z., and Ander, B.P. (2012). Cell cycle inhibition without disruption of neurogenesis is a strategy for treatment of aberrant cell cycle diseases: an update. ScientificWorldJournal 2012, 491737.
39. Liu, D., and Ander, B. (2011). Cell cycle phase transitions: signposts for aberrant cell cycle reentry in dying mature neurons. J. Cytol. Histol. 2, 5.
40. Liu, D., and Sharp, F. (2011). The dual role of SRC kinases in intracerebral hemorrhage. Acta Neurochir. Suppl. 111, 77–81.
41. Liu, Y., Wong, T.P., Aarts, M., Rooyakkers, A., Liu, L., Lai, T.W., Wu, D.C., Lu, J., Tymianski, M., Craig, A.M., and Wang, Y.T. (2007). NMDA receptor subunits have differential roles in mediating excitotoxic neuronal death both in vitro and in vivo. J. Neurosci. 27, 2846–2857.
42. Ardizzone, T.D., Lu, A., Wagner, K.R., Tang, Y., Ran, R., and Sharp, F.R. (2004).Glutamate receptor blockade attenuates glucose hypermetabolism in perihematomal brain after experimental intracerebral hemorrhage in rat. Stroke 35, 2587–2591.
43. Ardizzone, T.D., Zhan, X., Ander, B.P., and Sharp, F.R. (2007). SRC kinase inhibition improves acute outcomes after experimental intracerebral hemorrhage. Stroke 38, 1621–1625.
44. Chevaleyre, V., and Siegelbaum, S.A. (2010). Strong CA2 pyramidal neuron synapses define a powerful disynaptic cortico-hippocampal loop. Neuron 66, 560–572.
45. Dixon, C.E., Lyeth, B.G., Povlishock, J.T., Findling, R.L., Hamm, R.J., Marmarou, A., Young, H.F., and Hayes, R.L. (1987). A fluid percussion model of experimental brain injury in the rat. J. Neurosurg. 67, 110–119.
46. McIntosh, T.K., Vink, R., Noble, L., Yamakami, I., Fernyak, S., Soares, H., and Faden, A.L. (1989). Traumatic brain injury in the rat: characterization of a lateral fluid-percussion model. Neuroscience 28, 233–244.
47. Mahat, M., Fakrudeen Ali Ahamed, N., Chandrasekaran, S., Rajagopal, S., Narayanan, S., and Surendran, N. (2012). An improved method of transcutaneous cisterna magna puncture for cerebrospinal fluid sampling in rats. J. Neurosci. Methods 211, 272–279.
48. Sharma, A.K., Schultze, A.E., Cooper, D.M., Reams, R.Y., Jordan, W.H., and Snyder, P.W. (2006). Development of a percutaneous cerebrospinal fluid collection technique in F-344 rats and evaluation of cell counts and total protein concentrations. Toxicol. Pathol. 34, 393–395.
49. Pegg, C.C., He, C., Stroink, A.R., Kattner, K.A., and Wang, C.X. (2010).Technique for collection of cerebrospinal fluid from the cisterna magna in rat. J. Neurosci. Methods 187, 8–12.
50. Morris, R. (1984). Developments of a water-maze procedure for studying spatial learning in the rat. J. Neurosci. Methods 11, 47–60.
51. Lee, L.L., Galo, E., Lyeth, B.G., Muizelaar, J.P., and Berman, R.F. (2004). Neuroprotection in the rat lateral fluid percussion model of traumatic brain injury by SNX-185, an N-type voltage-gated calcium channel blocker. Exp. Neurol. 190, 70–78.
52. Wallace, W.J., Houtchens, R.A., Maxwell, J.C., and Caughey, W.S. (1982). Mechanism of autooxidation for hemoglobins and myoglobins. Promotion of superoxide production by protons and anions. J. Biol. Chem. 257, 4966–4977.
53. Lok, J., Leung, W., Murphy, S., Butler, W., Noviski, N., and Lo, E. (2011). Intracranial hemorrhage: mechanisms of secondary brain injury. Acta Neurochir. Suppl. 111, 63–69.
54. Misra, A., Ganesh, S., Shahiwala, A., and Shah, S.P. (2003). Drug delivery to the central nervous system: a review. J. Pharm. Pharm. Sc. 6, 252–273.
55. Albert-Weissenberger, C., and Siren, A.L. (2010). Experimental traumatic brain injury. Exp. Transl. Stroke Med. 2, 16.
56. Cortez, S.C., McIntosh, T.K., and Noble, L.J. (1989). Experimental fluid percussion brain injury: vascular disruption and neuronal and glial alterations. Brain Res. 482, 271–282.
57. Parsons, S.J., and Parsons, J.T. (2004). Src family kinases, key regulators of signal transduction. Oncogene 23, 7906–7909.
58. Cooke, M.P., and Perlmutter, R.M. (1989). Expression of a novel form of the fyn proto-oncogene in hematopoietic cells. New Biol. 1, 66–74.

59. Umemori, H., Wanaka, A., Kato, H., Takeuchi, M., Tohyama, M., and Yamamoto, T. (1992). Specific expressions of Fyn and Lyn, lymphocyte antigen receptor-associated tyrosine kinases, in the central nervous system. Brain Res. Mol. Brain Res. 16, 303–310.
60. Tang, H., Hao, Q., Rutherford, S.A., Low, B., and Zhao, Z.J. (2005). Inactivation of SRC family tyrosine kinases by reactive oxygen species in vivo. J. Biol. Chem. 280, 23918–23925.
61. Place, A.T., Chen, Z., Bakhshi, F.R., Liu, G., O'Bryan, J.P., and Minshall, R.D. (2011). Cooperative role of caveolin-1 and C-terminal Src kinase binding protein in C-terminal Src kinase-mediated negative regulation of c-Src. Mol. Pharmacol. 80, 665–672,
62. Kaimachnikov, N.P., and Kholodenko, B.N. (2009). Toggle switches, pulses and oscillations are intrinsic properties of the Src activation/deactivation cycle. FEBS J. 276, 4102–4118.
63. Kubier, A., and O'Brien, M. (2012). Endogenous anticoagulants. Top. Companion Anim. Med. 27, 81–87.
64. Lowell, C., and Soriano, P. (1996). Knockouts of Src-family kinases: stiff bones, wimpy T cells, and bad memories. Genes Dev. 10, 1845–1857.
65. Shimizu, A., Maruyama, T., Tamaki, K., Uchida, H., Asada, H., and Yoshimura, Y. (2005). Impairment of decidualization in SRC-deficient mice. Biol. Reprod. 73, 1219–1227.
66. Watkin, H., Richert, M.M., Lewis, A., Terrell, K., McManaman, J.P,, and Anderson, S.M. (2008). Lactation failure in Src knockout mice is due to impaired secretory activation. BMC Dev. Biol. 8, 6.

Address correspondence to:
Da Zhi Liu, PhD
Department of Neurology and M.I.N.D Institute
University of California at Davis Medical Center
2805 50th Street
Sacramento, CA 95817

E-mail: dzliu@ucdavis.edu